



Assessment of Aluminum Alloy 6351 Eggshell Reinforced Composite in Dry Turning Using Response Surface Methodology

S. C. Nwoziri ^a, Bethel Mba ^{b*}, Franklin Onwuka ^c,
E. B. Agbonko ^a, Uchenna Alozie ^d, Clifford Omonini ^e
and G. A Ogban-Ekpe ^a

^a Department of Mechanical Engineering, University of Calabar, Nigeria.

^b Department of Mechanical Engineering, Michael Okpara University of Agriculture Umudike, Nigeria.

^c Department of Mechanical Engineering, Federal University of Nigeria Nsukka, Nigeria.

^d Department of Mechanical Engineering, Federal Polytechnic Nekede, Nigeria.

^e Department of Mechanical and Aerospace Engineering, Nazarbayev University Astana, Kazakhstan.

Authors' contributions

This work was carried out in collaboration among all authors. All authors read and approved the final manuscript.

Article Information

DOI: <https://doi.org/10.56557/jobari/2024/v30i48840>

Open Peer Review History:

This journal follows the Advanced Open Peer Review policy. Identity of the Reviewers, Editor(s) and additional Reviewers, peer review comments, different versions of the manuscript, comments of the editors, etc are available here:

<https://prh.ikpress.org/review-history/12375>

Original Research Article

Received: 25/06/2024

Accepted: 29/08/2024

Published: 04/09/2024

ABSTRACT

Lack of knowledge and comprehension of critical input parameters and material machinability has limited the industry's use of machining, making it challenging to meet requirements for machining responses and numerous other problems. This study uses response surface methods to evaluate

*Corresponding author: E-mail: mbabethelchidiadi@gmail.com;

Cite as: Nwoziri, S. C., Bethel Mba, Franklin Onwuka, E. B. Agbonko, Uchenna Alozie, Clifford Omonini, and G. A Ogban-Ekpe. 2024. "Assessment of Aluminum Alloy 6351 Eggshell Reinforced Composite in Dry Turning Using Response Surface Methodology". *Journal of Basic and Applied Research International* 30 (4):43-60.
<https://doi.org/10.56557/jobari/2024/v30i48840>.

Aluminum Alloy 6351 Eggshell Reinforced Composite as a turning machining material. The material removal rate (MRR), cutting force (F_c), and surface roughness (Ra) of the samples were examined. The mass percentage of the composite is 15% egg shell reinforcement and 85% aluminum alloy. Cutting force (F_c), surface roughness (Ra), and material removal rate (MRR) ANOVA tables show that several models have significant probability values (P-values) less than 0.05. Numerical optimization was used to identify combinations of process parameters that will give the best response of cutting force (F_c), surface roughness (Ra), and material removal rate (MRR). The Cutting force (F_c), surface roughness (Ra), and material removal rate (MRR) can all be predicted using the regression equation model that was created. The only input variable that significantly affects the cutting force is cutting speed.

The three-input variable studied has a significant effect on surface roughness (Ra) and material removal rate (MRR).

The optimization result obtained indicates that the optimal response for turning an aluminum alloy 6351 eggshell reinforced composite is 1.39676 μ m, 101.333N, and 2016.77mm³/min for surface roughness (Ra), cutting force (F_c), and material removal rate (MRR), respectively. This is achieved when the input variables of cutting speed (V_c), feed rate (F_r), and depth of cut (D_c), which are 589.479 rpm, 0.205976 mm/min, and 0.315524 mm, respectively, are used.

Keywords: Numerical optimization; regression equation; material removal rate; surface roughness; cutting force.

ABBREVIATIONS

MRR	Material removal rate
AAERC	Aluminum alloy eggshell reinforced composite
AMMC	Aluminum metal matrix composites
BBD	Box-Behnken design
DOE	Design of experiment
Ra	Surface roughness
V_c	Cutting speed
F_c	Cutting force
D_c	Depth of cut
F_r	Feed rate

1. INTRODUCTION

CNC lathes have revolutionized the machining industry by automating turning processes. The computer numerical control lathe (CNC) is a type of machining tool that can be used to execute various operations on a workpiece. Among the several machining operations carried out by the CNC lathe, the most important operation is machine turning. Turning is one of the major machining techniques that is used to machine the outside diameter of a revolving cylindrical work piece [1,2]. Rotating the work item till it reaches a pre-established size can help to decrease its diameter through turning process. In order to obtain the desired diameter and reduce the diameter, the work item is frequently turned [3,4,5]. Parts that are cylindrical are created during the turning process [6,7]. Hence, it can be defined as the act of milling the outside of a work piece while it revolves in opposition to a cutting tool that is supplied perpendicular to the axis of the work piece.

The majority of operations requiring accuracy and surface smoothness use CNC. It is significant to note that the surface finish is impacted by the utilized operation speed [8-10]. V_c , D_c , and F_r being among the selected cutting parameters are utilized to create the expected response of MRR, F_c , and Ra [11-15]. The component's surface polish has been blamed for a variety of failures, some of which are catastrophic and cause enormous losses. In order to maximize the machining conditions and achieve a high surface polish, research has been developed for these reasons [16-22]. The measurement of a material's surface roughness is its micro-irregularities [23]. Many of a material's mechanical qualities, such as its capacity to withstand friction and wear, are predicted and determined by its surface roughness [16, 23-25]. When machining results in surface specification variations, high surface integrity may not be produced by finishing [26,27]. As a result, sufficient control measures must be taken to maintain surface roughness

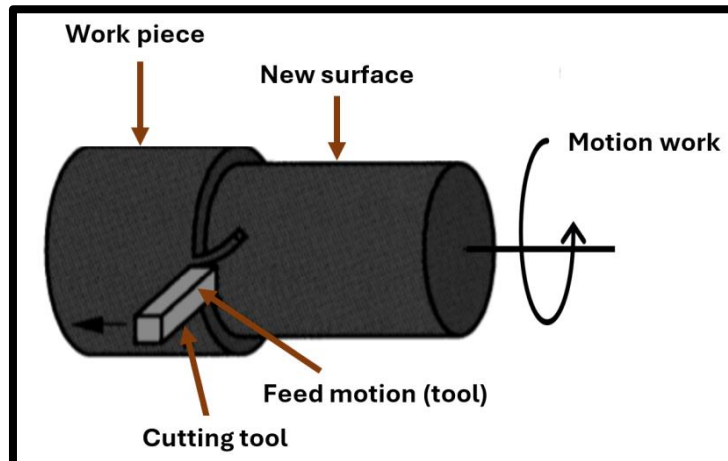


Fig. 1. Turning operation concept [76]

within allowable bounds, as this is a crucial criterion and technical prerequisite for assessing the quality of a product [28,29]. The tool shape, tool material, cutting condition, and finishing of the tool are some of the aspects that actually determine surface roughness [16]. V_c , D_c , and F_r are three key machining characteristics that affects the machined Ra [15]. The measured volume of the material removed or the weight difference between the initial and post-machining states can be used to calculate the material removal rate which is the amount of material removed from the workpiece in a certain amount of time [30]. To guarantee the best possible machined output, the MRR idea must be taken into account when developing metal cutting techniques and selecting cutting instruments [31-34]. The force generated by the cutting tool as it slices the workpiece is known as the cutting force. Machining errors can result from issues with the equipment, process, and procedures used in metal machining [35-37]. The main issues with machining operations are the mistakes brought on by strong cutting force [38-41]. As a result, cutting force is now an essential factor to take into account to ensure a stable and effective machining operation [42-45].

Aluminum metal matrix composites (AMMC), are a valuable and quickly expanding material with strong mechanical and physical characteristics that make them ideal for a various technical application [46-52]. The exceptional mechanical and physical qualities of AMMC make them suitable materials for a wide range of applications [46-49, 53-57]. Reinforced metallic materials provide superior mechanical and chemical properties compared to ordinary

engineering materials [58,59]. Recently, interest has risen in creating composites using inexpensive and low-density reinforcements to achieve engineering aims and specific objectives [60-62]. Aluminum Matrix Composites (AMCs), having aluminum as a principal constituent, are a high performance, lightweight class of materials [7]. The reinforcement in AMCs can be continuous or discontinuous fibers, whiskers, or particles, with the highest significant dominant material [52,63,64]. Many composite materials used today are in line with applications needing the most outstanding levels of performance due to their performance, high availability, and affordability [65-67]. The matrix and reinforcement of the composite serve, respectively, to improve mechanical properties, facilitate load transmission, and ensure structural integrity [46-49, 53-55].

2. MATERIALS AND METHODS

2.1 Materials

The materials and equipment utilized to do this task included a veneer caliper, measuring tape, Aluminum Alloy 6351, eggshell waste, a dynamometer (XXR-UN01), a surface tester (Mitutoyo sj-210), and a CNC lathe machine (250 PCD Boxford CNC lathe machine). Fig. 2 to Fig. 7, shows the Eggshells, Eggshell powder, Aluminum Alloy 6351 eggshell composite, Mutotuyo surface measuring instrument, mechanical stirrer with furnace and CNC lathe tool dynamometer respectively. Table 1 and Table 2 shows chemical compositions and the mechanical properties of the Aluminum alloy 6351, respectively.



Fig. 2. Egg shells



Fig. 3. Egg shell powder

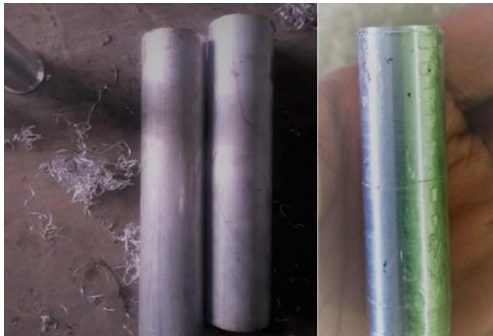


Fig. 4. Aluminum alloy 6351 eggshell composite



Fig. 5. Mutotuyo surface measuring instrument



Fig. 6. Mechanical Stirring with furnace



Fig. 7. CNC lathe tool dynamometer

Table 1. Composition of the A6351 alloy

Al	Si	Fe	Cu	Mn	Mg	Zn	Ti	V
Bal	7.0	0.1	0.002	0.006	0.4	0	0.13	0.02

Table 2. Mechanical properties of Al-6351 alloy

Sample	Specimen	Toughness (Joules)	Hardness (BHN)
1	Al-6351	6.638	60

2.2 Methods

2.2.1 Aluminum Alloy 6351 eggshell reinforced composite preparation

The egg shells were collected and cleaned to remove the dust and particles after which they

were washed thoroughly with water and allowed to dry in an oven heated to a temperature of 1000°C for a period of one hour. The desiccated egg shells were crushed and pulverized to room temperature to obtain the desired and finest crushed particle [68]. The resulting powder was passed through the necessary size sieves (>106

to <850 microns) to produce particles with a consistent size distribution. The composite composition by mass contained 85% Aluminum alloy and 15% Egg shell reinforcement [68]. The weights of the reinforcements (pulverized egg shell) were determined using electronic compact scale. The sourced Aluminum weight for the composite was determined using a weighing balance. The patterns used were made of wood while natural sand was used to prepare the sand mold.

Required amount of pulverized egg shell was kept in a furnace preheated in order to improve wettability [68]. A temperature probe was affixed to the aluminum to ensure total melting after the metal was heated to $700^{\circ}\text{C} \pm 50^{\circ}\text{C}$ in a diesel-powered crucible furnace. After being heated to a temperature of around 600°C , the liquid aluminum was carefully deposited into the furnace to achieve a semi-solid condition [69]. To further increase the metal's wettability by lowering surface tension, raising surface energy, and lowering matrix reinforcement interface energy, magnesium powder (2%) was first added to the molten metal [70-73]. The heated, grounded egg shell particles were charged into the semi-solid melt at different temperatures and stirring intervals [68]. An automatic mechanical stirrer was used to stir the semi-solid composite mixture after it had been superheated to $750^{\circ}\text{C} \pm 50^{\circ}\text{C}$ [68, 74,75]. To create sound castings, the fluid was then put into a sand mold and let to set.

2.2.2 Design of experiment

The objective of the experimental design was to choose the machining settings for 15 runs using three levels and three components at random value combinations.

The goal of the studies was to find the ideal V_c , D_c , and F_r combination as input variables to generate the best possible MRR, F_c , and Ra. The desired experimental design's focal point was replicated three times in 15 runs using the Box-Behnken design (BBD) experimental design.

The machining process variables and their levels are given in Table 3.

2.2.3 Experimental set up

Experiments on orthogonal turning was carried out on the 250 PCD Boxford CNC lathe machine multitasking machine tool at the University of Nigeria, LNG laboratory. The X, Y, and Z axes can all be linearly moved by the tool spindle. This arrangement made it simple to turn this machine and execute other tasks.

Cylindrical work piece of Aluminum Alloy 6351 eggshell composite of $\varnothing 220$ mm diameter is fixed between the three jaws of the universal chuck. The three primary control variables chosen for this investigation are the V_c , D_c , and F_r . The performed experimental trials were carried out at various combinations of input variables (V_c , D_c , and F_r). For each trial, values for MRR, F_c , and Ra were accurately recorded. Ensuring the accuracy of the turning process model requires careful consideration of selected factors.

2.2.4 Cutting operation procedures

The first turning operation on the CNC lathe was used to cut the AAERC to the required diameter of 220 mm for each of the several samples.

AAERCs were turned to the required diameter of 220 mm for each of the samples using a CNC lathe. Process control parameters such as V_c , D_c , and F_r are combined to commence turning machining using DOE. Different machining settings are tested in order to obtain desired levels of MRR, F_c , and Ra. The chuck was fastened with the work material centered. The tool holder was secured with the HSS cutting insert, and the required adjustments were done. F_c , and Ra were measured using a dynamometer and surface roughness tester (mitutoyo 2j-210) respectively. Fig. 8 and Fig. 9 shows the experimental setup and machined Aluminum Alloy 6351 reinforced composite respectively.

Table 3. Independent process variable and design levels

Variables	Units	Low (-1)	Medium (0)	High (+1)
V_c	Rpm	180	450	720
F_r	mm/rev	0.2	0.3	0.4
D_c	Mm	0.2	0.4	0.6



Fig. 8. Experimental setup (CNC lathe)



Fig. 9. Al. A6351 Eggshell machined sample

3. RESULTS AND DISCUSSION

This study explores the assessment of Aluminum Alloy 6351 eggshell reinforced composite as turning machining material using RSM. The impact of V_C , D_C , and F_r on the response were conducted on the material utilizing machining turning process. The design of experiment utilizes 3 level and 3 factors of box-Behnken design (BBD).

RSM combines statistical and mathematical techniques. Utilizing RSM to create continuous variable surfaces, assess response variables and interactions, and identify the optimal level range,

this study examines the optimization of machining parameters of Aluminum Alloy 6351 eggshell reinforced composite.

A regression equation was fitted to describe the functional relationship between components and responses, and the optimal process parameters were ascertained by analyzing the regression equation, which was created using the DOE in a fair test by RSM. The second order of analytical process parameters was resolved by this method, which is the multivariate optimization.

Table 4 show the final data for the actual design after experiment conducted.

Table 4. Final data table of the actual design after experiment.

Runs	V_C (rpm)	F_r (mm/min)	D_C (mm)	Ra (μm)	F_C (N)	MRR (mm^3/min)
1	180	0.2	0.4	1.16	171.2	2493.09
2	720	0.3	0.2	0.98	61.1	601.13
3	450	0.2	0.6	2.88	137.2	2488.45
4	720	0.2	0.4	2.12	95	1854.32
5	720	0.3	0.6	3.33	85.9	835.42
6	720	0.4	0.4	3.48	94.5	844.56
7	450	0.3	0.4	1.74	124.3	1516.4
8	450	0.4	0.2	1.14	119.7	735.8
9	180	0.3	0.6	2.9	169.7	1531.31
10	450	0.4	0.6	3.24	129.7	2352.69
11	450	0.3	0.4	1.38	130.2	1588.37
12	180	0.4	0.2	0.92	183.6	895.9
13	450	0.3	0.2	0.74	140	860.58
14	180	0.3	0.6	2.44	170.5	2237.11
15	450	0.2	0.2	0.9	115.3	1708.75

3.1 Quantitative assessment of F_C using ANOVA

Table 5 shows the analysis of variance of the F_C response to the Aluminum Alloy 6351 eggshell reinforced composite turning process. The model is considered significant with a P-value less than 0.00001 due to the study results demonstrating a non-significant lack of fit. The study indicates that V_C has a considerable impact on F_C during turning operations, as evidenced by the significant P-value of 0.0001. It is evident from the analysis of variance that this model is the most appropriate for response prediction because all mathematical models of F_C response have accuracy levels that surpass the 95%

confidence threshold. Tables 5, 6, and 7, displays the F_C response variance analysis table. R-square, R-square (adj), and predicted R-square have respective values of 0.9529, 0.9176, and 0.8141. The precision of the accepted mathematical model is supported by the near proximity of all observed coefficients, R-sq, R-sq (adj), and predicted R-sq. The coefficient of determination, also known as the entity R-squared quantity, is further utilized to assess the RSM model's level of competency [54]. The generated mathematical model's adequacy is demonstrated by its R-squared values, which indicate how well the model fits the gathered data and how closely it approaches 1 [54].

Table 5. ANOVA table of F_C

Source	Sum of Squares	df	Mean Square	F-value	p-value	
Model	16617.38	6	2769.56	27.00	< 0.0001	significant
V_C	14891.61	1	14891.61	145.16	< 0.0001	
F_r	0.2560	1	0.2560	0.0025	0.9614	
D_C	160.28	1	160.28	1.56	0.2466	
$V_C \times F_r$	6.98	1	6.98	0.0681	0.8008	
$V_C \times D_C$	292.09	1	292.09	2.85	0.1300	
$F_r \times D_C$	43.39	1	43.39	0.4229	0.5337	
Residual	820.71	8	102.59			
Lack of Fit	802.99	6	133.83	15.10	0.0634	not significant
Pure Error	17.72	2	8.86			
Cor Total	17438.09	14				

Table 6. Fit statistics of F_C

Std. Dev.	10.13	R ²	0.9529
Mean	128.53	Adjusted R ²	0.9176
C.V. %	7.88	Predicted R ²	0.8141
		Adeq. Precision	16.0680

Table 7. Coefficients in terms of coded factors of F_C

Factor	Coefficient Estimate	df	Standard Error	95% CI Low	95% CI High	VIF
Intercept	128.86	1	2.66	122.72	135.01	
V_C	-44.93	1	3.73	-53.53	-36.33	1.08
F_r	0.1838	1	3.68	-8.30	8.67	1.06
D_C	4.14	1	3.31	-3.50	11.78	1.07
$V_C \times F_r$	-1.39	1	5.34	-13.70	10.92	1.11
$V_C \times D_C$	8.27	1	4.90	-3.03	19.58	1.16
$F_r \times D_C$	-3.20	1	4.92	-14.55	8.15	1.16

Coded equation

$$F_C = +128.86 - 44.93 V_C + 0.1838 F_r + 4.14 D_C - 1.39 V_C \times F_r + 8.27 V_C \times D_C - 3.20 F_r \times D_C \dots \dots (1)$$

F_C is predicted by entering the variables for V_C , D_C , and F_r into the equation that represents the coded equation of F_C . The procedure of comparing the factor coefficients of the components to ascertain their relative significance is made easier and more straightforward by the coded equation.

Actual equation

$$F_C = +196.32061 - 0.212203 V_C + 89.04748 F_r - 0.221121 D_C - (0.051575 V_C \times F_r) + (0.153182 V_C \times D_C) - (160.00341 F_r \times D_C) \dots \dots \dots (2)$$

The real parameters measured during the turning operation are V_C , D_C , and F_r for the actual equation. The coefficients show how the cutting force is impacted by each parameter and how those relationships work. When the real input values are available, the F_C can be predicted using the actual equation. These equations help in optimizing turning machining processes of the composite by predicting the F_C based on different parameter settings of V_C , D_C , and F_r .

Fig. 10. shows the graph of F_C of predicted value against actual value. The figure shows a scattered plot comparing the predicted values versus actual values for the F_C . Each point

represents a pair of actual and predicted values. The line, which displays the degree to which the expected and actual values agree, is indicated by the line connecting the points. The graph suggests that the model's predictions are quite accurate, as the points closely follow the line of best fit. Diagonal line represents perfect prediction, where predicted values match actual values exactly. Scatter Points shows color-coded based on the F_C , ranging from 61.1 (green) to 183.6 (red). The points are closely aligned with the diagonal line, indicating that the predictive model is quite accurate in estimating the F_C .

3.2 Quantitative assessment of MRR using ANOVA

Table 8 and Table 9 shows the analysis of variance and fit statistics table respectively. Table 8 demonstrates that the model is highly significant with a p-value of 0.0222, suggesting that the MRR is considerably influenced by the input variables (V_C , D_C , and F_r) taken into consideration. V_C , F_r and D_C are significant with a p-value of 0.0281, 0.0365 and 0.0070 respectively. The interactions of the input parameters like $F_r \times D_C$, $V_C \times F_r$ and $V_C \times D_C$ are not significant. However, the quadratic terms (V_C^2 , F_r^2 , and D_C^2) are not significant.

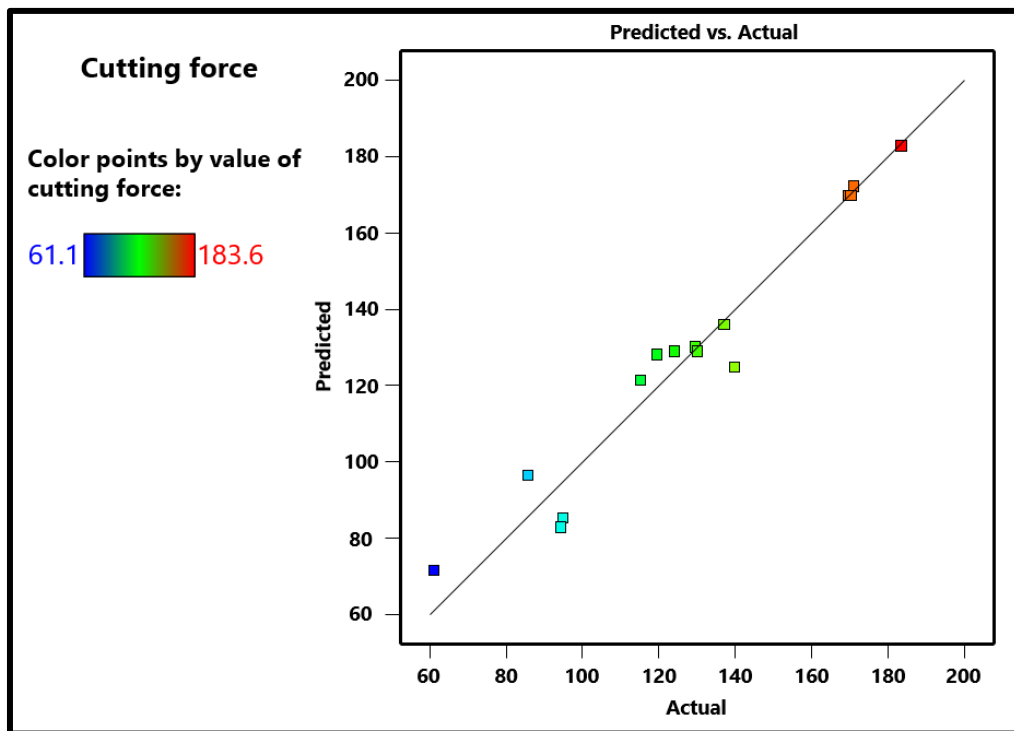


Fig. 10. Graph of predicted values and actual values of F_C .

The lack of fit is not significant, suggesting that the model fits the data adequately. Table 9 displays the model's fit to the data as a result of R² obtaining a value of 0.9271. The coefficient of determination, also known as the entity R-squared quantity, is further utilized to assess the RSM model's competency. The difference between the R² of 0.9271 and the Adjusted R² of 0.7958 is less than 0.2, indicating a reasonable level of agreement. The match between the created model and the collected data is better when the R-square is nearer 1 [54]. The R-

squared numbers demonstrate how well-developed the mathematical model is. There is an exceptional correlation between the independent variables, which is supported by the high values for all of the determination coefficients, which show that the modeling is highly significant. Table 10 shows that the MRR response mathematical models have accuracy levels in the analysis of variance that are greater than the 95% confidence level, suggesting that this model is the most suitable for response prediction.

Table 8. ANOVA table of MRR

Source	Sum of Squares	df	Mean Square	F-value	p-value	
Model	5.978E+06	9	6.643E+05	7.06	0.0222	significant
V_C	8.812E+05	1	8.812E+05	9.37	0.0281	
F_r	7.561E+05	1	7.561E+05	8.04	0.0365	
D_C	1.828E+06	1	1.828E+06	19.44	0.0070	
$V_C \times F_r$	54072.24	1	54072.24	0.5748	0.4825	
$V_C \times D_C$	1.436E+05	1	1.436E+05	1.53	0.2715	
$F_r \times D_C$	1.561E+05	1	1.561E+05	1.66	0.2540	
V_C^2	3.141E+05	1	3.141E+05	3.34	0.1272	
F_r^2	9.284E+05	1	9.284E+05	9.87	0.0256	
D_C^2	1.795E+05	1	1.795E+05	1.91	0.2257	
Residual	4.703E+05	5	94063.88			
Lack of Fit	2.187E+05	3	72884.24	0.5792	0.6830	not significant
Pure Error	2.517E+05	2	1.258E+05			
Cor Total	6.449E+06	14				

Table 9. Fit statistics of MRR

Std. Dev.	306.70	R²	0.9271
Mean	1502.93	Adjusted R ²	0.7958
C.V. %	20.41		

Table 10. Coefficients in terms of coded factors of MRR

Factor	Coefficient Estimate	df	Standard Error	95% CI Low	95% CI High	VIF
Intercept	1544.73	1	205.28	1017.04	2072.42	
V_C	-352.42	1	115.15	-648.41	-56.43	1.13
F_r	-326.05	1	115.00	-621.66	-30.43	1.12
D_C	454.72	1	103.14	189.59	719.85	1.13
$V_C \times F_r$	-129.97	1	171.42	-570.61	310.68	1.25
$V_C \times D_C$	-200.24	1	162.05	-616.80	216.33	1.38
$F_r \times D_C$	194.55	1	151.01	-193.64	582.75	1.20
V_C^2	-302.26	1	165.41	-727.47	122.95	1.09
F_r^2	545.40	1	173.60	99.14	991.66	1.20
D_C^2	-257.79	1	186.62	-737.52	221.94	1.23

Coded equation

$$MRR = +1544.73 - 352.42 V_C - 326.05 F_r + 454.72 D_C - 129.97 V_C \times F_r - 200.24 V_C \times D_C + 194.55 F_r \times D_C - 302.26 V_C^2 + 545.40 F_r^2 - 257.79 D_C^2 \dots \dots \dots (3)$$

The coding equation of MRR can be anticipated by plugging in the values for V_C , F_r and D_C . The coded equation facilitates and simplifies the process of comparing the component factor coefficients to determine their respective importance. Regression models with coded coefficients show how each element affects the response. Coded equations show which way the response optimum is sharpest in the case of first-order models. It is less difficult to deal with varied scales and units for each element when coded factors are used. We are able to compare factors on a common scale by using the coded equation as a standardizing technique.

Actual equation

$$\begin{aligned}
 MRR = & +5088.66895 + 5.35360 V_C - \\
 & 37709.43741 F_r + 6179.75057 D_C - \\
 & 4.81359 V_C \times F_r - 3.70806 V_C \times D_C + \\
 & 9727.61882 F_r \times D_C - 0.004146 V_C^2 + \\
 & 54540.08488 F_r^2 - \\
 & 6444.76595 D_C^2 \dots \dots \dots (4)
 \end{aligned}$$

The real parameters that are measured during the turning operation are V_C , F_r and D_C . The coefficients show how the various parameters and the MRR are correlated. When the actual input values are known, one can forecast the MRR using the actual equation. These formulas, which take into account different V_C , F_r and D_C

parameter values, can be used to anticipate the MRR for turning machining processes.

Simulation on how the response variable (output) and the actual factor levels relate to each other can be carried out using the actual equations. The response can be predicted for any given collection of factor values by fitting the model to the experimental data. When it comes to process optimization, this forecast aids in decision-making. The reaction can be maximized or minimized by using the actual formulae to determine the ideal factor choices. Techniques for optimization find the optimal factor levels by utilizing the equations. Strict formulas are necessary to attain the intended results. The impact of each factor is revealed by the coefficients in the real equations. While negative coefficients point to factors that may be reducing the response, positive coefficients show those that are increasing it.

The real equations aid in modifying factor concentrations to preserve intended response values.

The formulas can be used to calculate what needs to be adjusted if the answer diverges from the intended outcome. We are able to measure how sensitive the response is to each element thanks to the real formulae. Robust process design is guided by sensitive information.

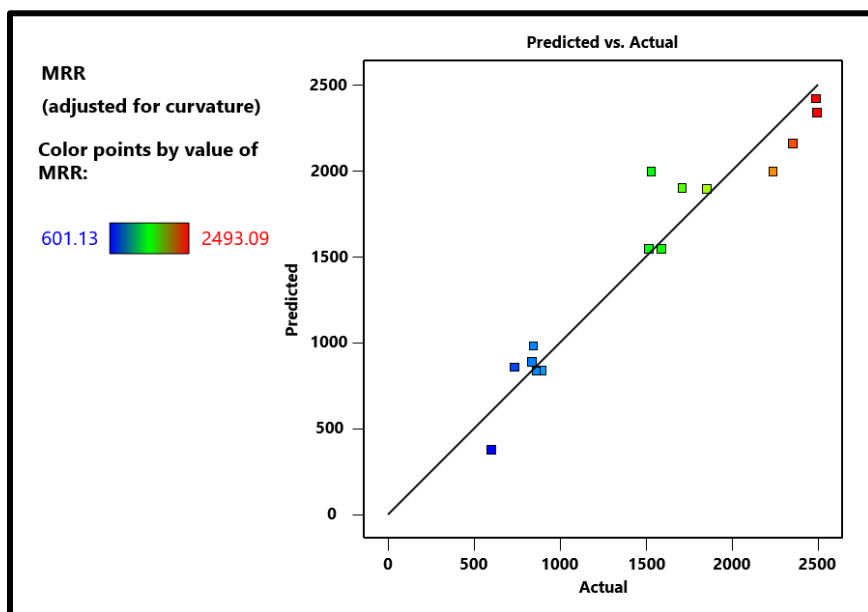


Fig. 11. Graph of predicted values and actual values of MRR

Fig. 11. shows the graph of MRR of predicted value against actual value. The MRR, which ranges from 601.13 (blue) to 2493.09 (red), is shown by a color gradient in the predicted vs. actual graph, which contrasts the predicted and actual values of a response variable. The diagonal line, which runs from lower left to upper right, shows the points in the data set where the anticipated and actual values exactly match. The accuracy of the predictions is indicated by the data points being dispersed about the diagonal line and better forecasts are shown by the points being closer to the line.

3.3 Quantitative assessment of Ra using ANOVA

Tables 11 and 12, respectively, present the fit statistics table and the analysis of variance table. The results presented indicate that the model has a p-value of less than 0.0001, indicating that

V_C , F_r and D_C have a substantial impact on the Ra rate. V_C , F_r and D_C , all have significant p-values of 0.0001, 0.0188, and 0.0049, respectively. The model appears to have an appropriate fit to the data, since the lack of fit is not statistically significant. The fits statistic reveals an R^2 value of 0.9001, indicating a very good fit between the model and the data. There is a fair agreement as the gap between the predicted R^2 of 0.8152 and the adjusted R^2 of 0.8729 is less than 0.2.

The adequate precision of 16.095, which is greater than 4, indicates that the signal intensity is adequate. A statistically significant lack of fit is indicated by a 1.62 F-value. Table 13 demonstrates that the model is the most suitable for Ra prediction, with all mathematical models for Ra responses exhibiting accuracy levels in the analysis of variance exceeding the 95% confidence level.

Table 11. ANOVA table of Ra

Source	Sum of Squares	df	Mean Square	F-value	p-value	
Model	12.75	3	4.25	33.04	< 0.0001	significant
V_C	1.58	1	1.58	12.30	0.0049	
F_r	0.9751	1	0.9751	7.58	0.0188	
D_C	11.60	1	11.60	90.21	< 0.0001	
Residual	1.41	11	0.1286			
Lack of Fit	1.24	9	0.1383	1.62	0.4391	not significant
Pure Error	0.1706	2	0.0853			
Cor Total	14.16	14				

Table 12. Fit statistics of Ra

Std. Dev.	0.3586	R^2	0.9001
Mean	1.96	Adjusted R^2	0.8729
C.V. %	18.33	Predicted R^2	0.8152
		Adeq. Precision	16.0947

Table 13. Coefficients in terms of coded factors of Ra

Factor	Coefficient Estimate	df	Standard Error	95% CI Low	95% CI High	VIF
Intercept	1.96	1	0.0926	1.75	2.16	
V_C	0.4476	1	0.1276	0.1667	0.7285	1.01
F_r	0.3514	1	0.1276	0.0705	0.6322	1.01
D_C	1.09	1	0.1149	0.8381	1.34	1.03

Coded equation

$$\text{Surface roughness (Ra)} = +1.96 + 0.4476 V_C + 0.3514 F_r + 1.09 D_C \dots \dots \dots (5)$$

The coding equation of Ra can be anticipated by plugging in the values for V_C , F_r and D_C . The coded equation facilitates and simplifies the process of comparing the component factor coefficients to determine their respective importance. Regression models with coded coefficients show how each element affects the response. Coded equations show which way the response optimum is sharpest in the case of first-order models. It is less difficult to deal with varied scales and units for each element when coded factors are used. We are able to compare factors on a common scale by using the coded equation as a standardizing technique.

Actual equation

$$\text{Surface roughness (Ra)} = -2.02524 + 0.001658 V_C + 3.51362 F_r + 5.45449 D_C \dots (6)$$

The actual parameters that are measured in a turning process are the V_C , F_r and D_C . The correlation between the Ra and the different parameters is displayed by the coefficients. One can use the actual equation to forecast the Ra when the actual input values are known. The Ra for turning composite machining operations can be predicted using these formulas, which account for various V_C , F_r and D_C parameter values.

The actual equations can be used to simulate the relationship between the response variable (output) and the actual factor values. The model can be fitted to the experimental data to predict the response for any given set of factor values.

This forecast helps with decision-making when it comes to process optimization. By figuring out the best factor selections using the actual equations, the response can be maximized or minimized. Equations are used by optimization techniques to determine the ideal factor levels. Tight formulations are required in order to achieve the desired outcomes. The coefficients in the actual equations show the effect of each element.

Positive coefficients indicate factors that are raising the reaction, while negative coefficients suggest those that might be decreasing it. To maintain the desired response values, factor concentrations can be changed with the use of the real equations. If the results deviate from what was planned, the formulas can be used to determine what has to be changed. The true equations allow us to quantify the response's sensitivity to each ingredient. Sensitive data serves as a roadmap for robust process design.

Fig. 12 shows the graph of Ra of predicted value against actual value. The Ra, which ranges from 0.74 (blue) to 3.48 (red), is shown by a color gradient in the predicted vs. actual graph, which contrasts the predicted and actual values of a response variable. The diagonal line, which runs from lower left to upper right, shows the points in the data set where the anticipated and actual values exactly match. The accuracy of the predictions is indicated by the data points being dispersed about the diagonal line and better forecasts are shown by the points being closer to the line.

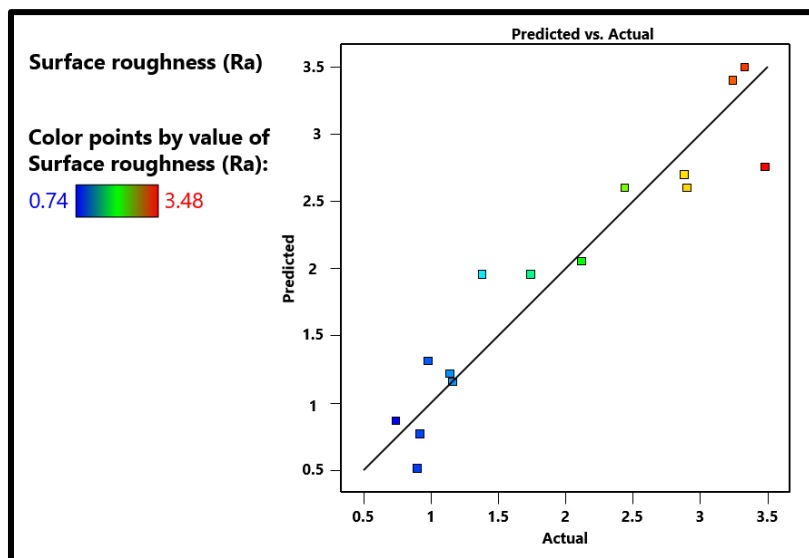


Fig. 12. Graph of predicted values and actual values of Ra.

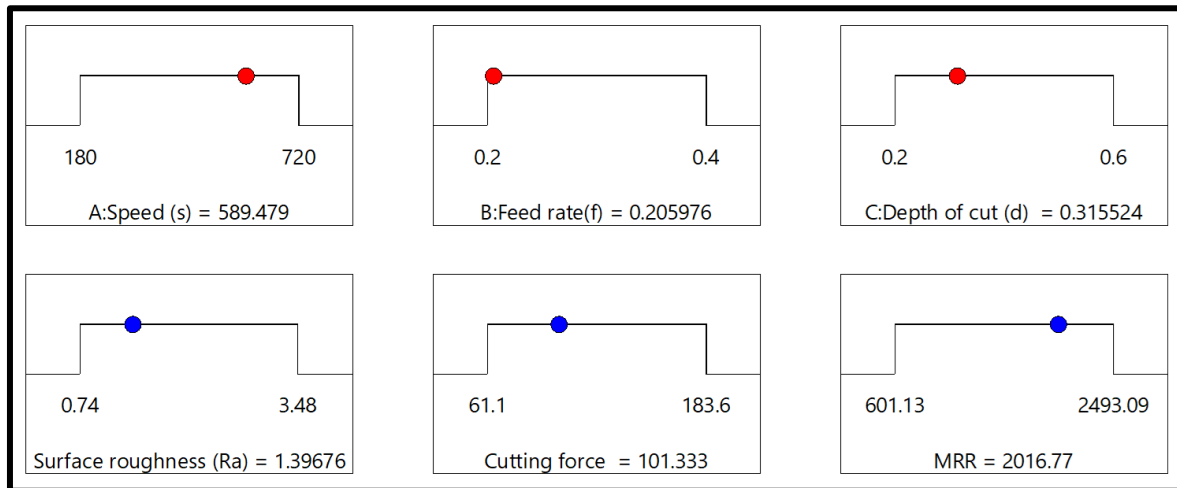


Fig. 13. Numerical optimization Aluminum Alloy 6351 Eggshell Reinforced Composite

3.4 Optimization using Numerical Method

Fig. 13. shows the numerical optimization of Aluminum Alloy 6351 Eggshell Reinforced Composite. Desirability function optimization is the process of finding an arrangement of input variables that are then utilized to collectively optimize a set of answers by meeting the needs of each response in the set. Response optimization is the function's main objective. Optimizing sets typically involves two goals: reducing the response or increasing it. Additionally, each response's single expected value is represented by a weighted geometric mean. The optimization of desirability functions involves forecasting and refining the response to achieve the best possible combination of desired parameters. This function accepts the predicted values for every reaction meter on a preferred, or least ideal to most ideal, scale that runs from 0 to 1. The desired values for the expected composite are obtained by combining a single expected value. The best input variable setting is found by maximizing the integrated expectation value. The study utilizes the numerical optimization technique which provides clear explanation to generate the optimal input combination that will give the best response. The optimization carried out utilizes the desirability function of 1 which is the first out of 100 solutions.

The optimization result carried out shows that when the input variables of V_c , F_r and D_c of 589.479rpm, 0.205976mm/min, and 0.315524mm respectively are utilized in performing turning operation on Aluminum Alloy 6351 Eggshell Reinforced Composite, the optimal response is obtained with the values of

R_a , F_c and MRR being 1.39676 μ m, 101.333N, and 2016.77mm³/min, respectively.

4. CONCLUSIONS

This paper examines the assessment of Aluminum Alloy 6351 eggshell reinforced composite as turning machining material using response surface methodology. The samples were investigated for R_a , MRR and F_c . The conclusion drawn from the evaluated results were as follows:

1. Aluminum Alloy 6351 eggshell reinforced composite was successfully utilized for this investigation.
2. Numerical optimization was used to identify combinations of process parameters that will give the best response of F_c , R_a , and MRR.
3. The F_c , R_a , and MRR can all be predicted using the regression equation model that was created.
4. V_c is the only factor that has a significant effect on the F_c . The three-input variable studied has a significant effect on R_a and MRR.
5. The optimization result obtained indicates that the optimal response for turning an Aluminum Alloy 6351 eggshell reinforced composite is 1.39676 μ m, 101.333N, and 2016.77mm³/min for R_a , F_c , and MRR, respectively. This is achieved when the input variables of V_c , F_r and D_c , which are 589.479 rpm, 0.205976 mm/min, and 0.315524 mm, respectively, are used.
6. The significance of this research is in its ability to furnish information regarding the

appropriate input parameters that must be employed to get the desired output parameters. By adjusting these settings, you may reduce material waste, increase energy efficiency, and get the optimum surface finishing.

DISCLAIMER (ARTIFICIAL INTELLIGENCE)

Author(s) hereby declares that NO generative AI technologies such as Large Language Models (ChatGPT, COPILOT, etc.) and text-to-image generators have been used during writing or editing of manuscripts.

COMPETING INTERESTS

Authors have declared that no competing interests exist.

REFERENCES

1. Vikram KA, Prasad RDV, Lakshmi VVK, Praveen AMV. Overview of turn-milling machining processes – A review. 2023;020011. Available: <https://doi.org/10.1063/5.0182884>
2. Yau LC, Chockalingam P. Material Removal Rate Study on Turning of Al Alloy. In: Proceedings of the Multimedia University Engineering Conference (MECON 2022). Atlantis Press International BV; 2023. p. 68–81. Available: https://doi.org/10.2991/978-94-6463-082-4_9
3. Butola R, Sharma V, Kanwar S, Tyagi L, Singari RM, Tyagi M. Optimizing the machining variables in CNC turning of aluminum-based hybrid metal matrix composites. SN Appl Sci. 2020;2(8):1356. Available: <https://doi.org/10.1007/s42452-020-3155-8>
4. Kumar MV, Kumar MP, Krishna SV, Kumar KV. Optimization of CNC Turning Parameters in Machining EN19 using Face Centered Central Composite Design Based RSM. Int J Recent Technol Eng. 2020;9(2):889–96. Available: <https://doi.org/10.35940/ijrte.B3923.079220>
5. Santhosh AJ, Tura AD, Jiregna IT, Gemechu WF, Ashok N, Ponnusamy M. Optimization of CNC turning parameters using face centred CCD approach in RSM and ANN-genetic algorithm for AISI 4340 alloy steel. Results Eng. 2021;11:100251. Available: <https://doi.org/10.1016/j.rineng.2021.100251>
6. Gnanavelbabu A, Arunachalam V, Sunu Surendran KT, Rajkumar K. Optimization of machining parameters in CNC turning of AA6061-B4C-CNT hybrid composites using Grey-fuzzy method. IOP Conf Ser Mater Sci Eng. 2020;764(1):012010. Available: <https://doi.org/10.1088/1757-899X/764/1/012010>
7. Srinivasan V, Kunjiappan S, Palanisamy P. A brief review of carbon nanotube reinforced metal matrix composites for aerospace and defense applications. Int Nano Lett. 2021;11(4):321–45. Available: <https://doi.org/10.1007/s40089-021-00328-y>
8. Akhtar MN, Sathish T, Mohanavel V, Afzal A, Arul K, Ravichandran M, Rahim IA, Alhady SSN, Bakar EA, Saleh B. Optimization of Process Parameters in CNC Turning of Aluminum 7075 Alloy Using L27 Array-Based Taguchi Method. Materials. 2021;14(16):4470. Available: <https://doi.org/10.3390/ma14164470>
9. Nataraj M, Balasubramanian K. Parametric optimization of CNC turning process for hybrid metal matrix composite. Int J Adv Manuf Technol. 2017;93(1–4):215–24. Available: <https://doi.org/10.1007/s00170-016-8780-4>
10. Saini P, Singh PK. Characterization and optimization analysis on surface finish and energy consumption in turning of Al-4032/GMP MMC produced by stir casting. Proc Inst Mech Eng Part C J Mech Eng Sci. 2022;236(24):11549–63. Available: <https://doi.org/10.1177/09544062221110475>
11. Arun Ramnath R, Thyla P, Mahendra Kumar N, Aravind S. Optimization of machining parameters of composites using multi-attribute decision-making techniques: A review. J Reinforced Plastics Composites. 2018;37(2):77–89. Available: <https://doi.org/10.1177/0731684417732840>
12. Gangwar S, Mondal SC, Kumar A, Ghadai RK. Performance analysis and optimization of machining parameters using coated tungsten carbide cutting tool developed by novel S3P coating method. Int J Interact Des Manuf (IJIDeM). 2024. Available: <https://doi.org/10.1007/s12008-024-01852-9>

13. Jamaludin Z, Shamshol Ali NA, Rafan NA, Abdullah L. Effect of Cutting Forces on Surface Roughness for Varying Depth of Cut and Feed Rates in Milling Machining Process. 2020. p. 195–203. Available: https://doi.org/10.1007/978-981-13-9539-0_20
14. Rajendra B, Deepak D. Optimization of Process Parameters for Increasing Material Removal Rate for Turning Al6061 Using S/N Ratio. *Procedia Technol.* 2016;24:399–405. Available: <https://doi.org/10.1016/j.protcy.2016.05.055>
15. Tefera AG, Sinha DK, Gupta G. Experimental investigation and optimization of cutting parameters during dry turning process of copper alloy. *J Eng Appl Sci.* 2023;70(1):145. Available: <https://doi.org/10.1186/s44147-023-00314-5>
16. Abellán-Nebot JV, Vila Pastor C, Siller HR. A Review of the Factors Influencing Surface Roughness in Machining and Their Impact on Sustainability. *Sustainability.* 2024;16(5):1917. Available: <https://doi.org/10.3390/su16051917>
17. González G, Schulze V. Surface conditioning in machining: optimizing component performance through advanced process modeling and control. *Prod Eng.* 2024;18(2):193–6. Available: <https://doi.org/10.1007/s11740-024-01268-0>
18. Guleria V, Kumar V, Singh PK. Recent Trends in the Amelioration and Prediction of Surface Roughness in Turning Process: A Bibliometric Analysis. 2023. p. 77–90. Available: https://doi.org/10.1007/978-981-19-4208-2_7
19. Kamguem R, Djebara A, Songmene V. Investigation on surface finish and metallic particle emission during machining of aluminum alloys using response surface methodology and desirability functions. *Int J Adv Manuf Technol.* 2013;69(5–8):1283–98. Available: <https://doi.org/10.1007/s00170-013-5105-8>
20. la Monaca A, Murray JW, Liao Z, Speidel A, Robles-Linares JA, Axinte DA, Hardy MC, Clare AT. Surface integrity in metal machining - Part II: Functional performance. *Int J Mach Tools Manuf.* 2021;164:103718. Available: <https://doi.org/10.1016/j.ijmactools.2021.103718>
21. Micallef C, Zhuk Y, Aria AI. Recent Progress in Precision Machining and Surface Finishing of Tungsten Carbide Hard Composite Coatings. *Coatings.* 2020;10(8):731. Available: <https://doi.org/10.3390/coatings10080731>
22. Zeidler H, Boettger-Hiller F, Edelmann J, Schubert A. Surface Finish Machining of Medical Parts Using Plasma Electrolytic Polishing. *Procedia CIRP.* 2016;49:83–7. Available: <https://doi.org/10.1016/j.procir.2015.07.038>
23. Aghababaei R, Brodsky EE, Molinari J-F, Chandrasekar S. How roughness emerges on natural and engineered surfaces. *MRS Bull.* 2022;47(12):1229–36. Available: <https://doi.org/10.1557/s43577-022-00469-1>
24. Bañón-García F, Bermudo Gamboa C, López-Fernández JA, Trujillo-Vilches FJ, Martín-Béjar S. Correlation between Surface Texture, Wettability and Mechanical Strength of Poly(lactic Acid) Parts Fabricated by Fused Filament Fabrication. *Coatings.* 2024;14(8):1033. Available: <https://doi.org/10.3390/coatings14081033>
25. Magsipoc E, Zhao Q, Grasselli G. 2D and 3D Roughness Characterization. *Rock Mech Rock Eng.* 2020;53(3):1495–519. Available: <https://doi.org/10.1007/s00603-019-01977-4>
26. Pimenov DY, Kiran M, Khanna N, Pintaude G, Vasco MC, da Silva LRR, Giasin K. Review of improvement of machinability and surface integrity in machining on aluminum alloys. *Int J Adv Manuf Technol.* 2023;129(11–12):4743–79. Available: <https://doi.org/10.1007/s00170-023-12630-4>
27. Wu D, Liu S, Wang H. High surface integrity machining of typical aviation difficult-to-machine material blade. *Int J Adv Manuf Technol.* 2023;129(7–8):2861–73. Available: <https://doi.org/10.1007/s00170-023-12533-4>
28. Ružbarský J. Roughness Control of Surfaces Using a Laser Profilometer with the Selected Material Cutting Technology. *Materials.* 2023;16(11):4109. Available: <https://doi.org/10.3390/ma16114109>

29. Shao M, Xu D, Li S, Zuo X, Chen C, Peng G, Zhang J, Wang X, Yang Q. A review of surface roughness measurements based on laser speckle method. *J Iron Steel Res Int.* 2023;30(10):1897–915. Available: <https://doi.org/10.1007/s42243-023-00930-8>
30. Liao Z, la Monaca A, Murray J, Speidel A, Ushmaev D, Clare A, Axinte D, M'Saoubi R. Surface integrity in metal machining - Part I: Fundamentals of surface characteristics and formation mechanisms. *Int J Mach Tools Manuf.* 2021;162:103687. Available:<https://doi.org/10.1016/j.ijmachtools.2020.103687>
31. Bilal A, Perveen A, Talamona D, Jahan MP. Understanding material removal mechanism and effects of machining parameters during EDM of zirconia-toughened alumina ceramic. *Micromachines.* 2021;12(1):67. DOI:10.3390/mi12010067.
32. Cao H, Zhou K, Chen X. Stability-based selection of cutting parameters to increase material removal rate in high-speed machining process. *Proc Inst Mech Eng [Part B].* 2016;230(2):227–40. DOI:10.1177/0954405415617931.
33. Navaneethan G, Palanisamy S, Jayaraman PP, Kang Y-B, Stephens G, Papageorgiou A, Navarro J. A review of automated cutting tool selection methods. *Int J Adv Manuf Technol.* 2024;133(3–4):1063–82. DOI:10.1007/s00170-024-13823-1.
34. Wang B, Liu Z, Cai Y, Luo X, Ma H, Song Q, Xiong Z. Advancements in material removal mechanism and surface integrity of high-speed metal cutting: A review. *Int J Mach Tools Manuf.* 2021;166:103744. DOI:10.1016/j.ijmachtools.2021.103744.
35. Astakhov VP. Cutting force modeling: Genesis, state of the art, and development. In: Astakhov VP, editor. *Cutting force modeling: Genesis, state of the art, and development.* 2022. p. 39–93. DOI:10.1007/978-3-030-90487-6_2.
36. Monroy Vazquez KP, Giardini C, Ceretti E. Cutting force modeling. In: *CIRP Encyclopedia of Production Engineering.* Springer Berlin Heidelberg; 2014. p. 315–9. DOI:10.1007/978-3-642-20617-7_6399.
37. Monroy Vazquez KP, Giardini C, Ceretti E. Cutting force modeling. In: *CIRP Encyclopedia of Production Engineering.* Springer Berlin Heidelberg; 2019. p. 417–32. DOI:10.1007/978-3-662-53120-4_6399.
38. Lee S, Jo W, Kim H, Koo J, Kim D. Deep learning-based cutting force prediction for machining process using monitoring data. *Pattern Anal Appl.* 2023;26(3):1013–25. doi:10.1007/s10044-023-01143-1.
39. Liu M, Xie H, Pan W, Ding S, Li G. Prediction of cutting force via machine learning: state of the art, challenges and potentials. *J Intell Manuf.* 2023. DOI:10.1007/s10845-023-02260-8.
40. Radu P, Schnakovszky C. A review of proposed models for cutting force prediction in milling parts with low rigidity. *Machines.* 2024;12(2):140. DOI:10.3390/machines12020140.
41. Yousefian O, Balabokhin A, Tarbuton J. Point-by-point prediction of cutting force in 3-axis CNC milling machines through voxel framework in digital manufacturing. *J Intell Manuf.* 2020;31(1):215–26. DOI:10.1007/s10845-018-1442-7.
42. Charalampous P. Prediction of cutting forces in milling using machine learning algorithms and finite element analysis. *J Mater Eng Perform.* 2021;30(3):2002–13. DOI:10.1007/s11665-021-05507-8.
43. Dubey V, Sharma AK, Kumar H, Arora PK. Prediction of cutting forces in MQL turning of AISI 304 Steel using machine learning algorithm. *J Eng Res.* 2022. DOI:10.36909/jer.ICMET.17177.
44. Khelifi H, Abdellaoui L, Bouzid Saï W. Prediction of cutting force and surface roughness in turning using machine learning. In: *Advances in Mechanical Engineering.* 2024. p. 213–22. DOI:10.1007/978-3-031-42659-9_24.
45. Sujuan W, Tao Z, Wenping D, Zhanwen S, To S. Analytical modeling and prediction of cutting forces in orthogonal turning: a review. *Int J Adv Manuf Technol.* 2022;119(3–4):1407–34. DOI:10.1007/s00170-021-08114-y.
46. Kumar A, Singh VP, Singh RC, Chaudhary R, Kumar D, Mourad AH. A review of aluminum metal matrix composites: fabrication route, reinforcements, microstructural, mechanical, and corrosion properties. *J Mater Sci.* 2024;59(7):2644–711. DOI:10.1007/s10853-024-09398-7.
47. Pattar J, Ramesh D, Malghan RL, Kumar A, Kumar P, H M V. Investigation of AA6063-based metal–matrix composites

- reinforced with TiO₂ dispersoids through digitally assisted techniques for mechanical, tribological, and microstructural characterizations. *Front Mech Eng.* 2024;10.
DOI:10.3389/fmech.2024.1393959.
48. Samuel Ratna Kumar PS, Mashinini PM. Laser additive manufacturing of aluminium matrix composites. In: *Advances in Manufacturing and Processing*. 2022. p. 73–90.
DOI:10.1007/978-3-030-89401-6_4.
49. Wazeer A, Mukherjee A, Das A, Sengupta B, Mandal G, Sinha A. Mechanical properties of aluminium metal matrix composites: advancements, opportunities and perspective. In: *Advances in Metal Matrix Composites*. 2024. p. 145–60.
DOI:10.1007/978-981-99-5982-2_9.
50. Aynalem GF. Processing methods and mechanical properties of aluminium matrix composites. *Adv Mater Sci Eng.* 2020;2020:1–19.
DOI:10.1155/2020/3765791.
51. Panchal GR, Srinath MS. Development of aluminum matrix composite through microwave stir casting. In: *Advances in Composite Materials*. 2021. p. 75–83.
DOI:10.1007/978-981-33-4018-3_7.
52. Su J, Teng J. Recent progress in graphene-reinforced aluminum matrix composites. *Front Mater Sci.* 2021;15(1):79–97.
DOI:10.1007/s11706-021-0541-0.
53. Laghari RA, Jamil M, Laghari AA, Khan AM, Akhtar SS, Mekid S. A critical review on tool wear mechanism and surface integrity aspects of SiCp/Al MMCs during turning: prospects and challenges. *Int J Adv Manuf Technol.* 2023;126(7–8):2825–62.
DOI:10.1007/s00170-023-11178-7.
54. Laghari RA, Li J. Modeling and optimization of cutting forces and effect of turning parameters on SiCp/Al 45% vs SiCp/Al 50% metal matrix composites: A comparative study. *SN Appl Sci.* 2021;3(7):706.
DOI:10.1007/s42452-021-04689-z.
55. Li J, Laghari RA. A review on machining and optimization of particle-reinforced metal matrix composites. *Int J Adv Manuf Technol.* 2019;100(9–12):2929–43.
DOI:10.1007/s00170-018-2837-5.
56. Wong WLE, Seetharaman S. Metal matrix composites. In: *Advances in Composite Materials*. 2021. p. 129–58.
DOI:10.1007/978-3-030-71438-3_6.
57. Zhou J, Li CJ, Li CX. Fabrication of metal matrix composites via high-speed particle implantation. *J Therm Spray Technol.* 2020;29(8):1910–25.
doi:10.1007/s11666-020-01106-6.
58. Manjunath R, Kumar D, Kumar A. A review on the significance of hybrid particulate reinforcements on the mechanical and tribological properties of stir-casted aluminum metal matrix composites. *J Bio-Tribo-Corrosion.* 2021;7(3):122.
DOI:10.1007/s40735-021-00558-9.
59. Srivastava A. Recent advances in metal matrix composites (MMCs): A review. *Biomed J Sci Technol Res.* 2017;1(2).
DOI:10.26717/BJSTR.2017.01.000236.
60. Abdur Rahman M, Haque S, Athikesavan MM, Kamaludeen MB. A review of environmentally friendly green composites: production methods, current progresses, and challenges. *Environ Sci Pollut Res.* 2023;30(7):16905–29.
DOI:10.1007/s11356-022-24879-5.
61. Crupi V, Epasto G, Napolitano F, Palomba G, Papa I, Russo P. Green composites for maritime engineering: A review. *J Mar Sci Eng.* 2023;11(3):599.
DOI:10.3390/jmse11030599.
62. Liu S, Liu L, Yang K, Yuan Z, Li X, Li C, Meng S. Reinforcing the mechanical properties of bamboo fiber/low density polyethylene composites with modified bamboo-woven structure. *J Mater Sci.* 2023;58(25):10359–69.
DOI:10.1007/s10853-023-08682-2.
63. Barot RP, Desai RP, Sutaria MP. Recycling of aluminium matrix composites (AMCs): A review and the way forward. *Int J Metal Casting.* 2023;17(3):1899–916.
DOI:10.1007/s40962-022-00905-7.
64. Mistry JM, Gohil PP. Research review of diversified reinforcement on aluminum metal matrix composites: fabrication processes and mechanical characterization. *Sci Eng Compos Mater.* 2018;25(4):633–47.
DOI:10.1515/secm-2016-0278.
65. Asyraf MR, Ilyas RA, Sapuan SM, Harussani MM, Hariz HM, Aiman JM, Baitaba DM, Sanjay MR, Ishak MR, Norkhairunnisa M, Sharma S, Alam MA, Asrofi M. Advanced composite in aerospace applications: Opportunities, challenges, and future perspective. In: *Advanced Composites in Aerospace*

- Engineering Applications. Springer International Publishing; 2022. p. 471–98. DOI:10.1007/978-3-030-88192-4_24.
66. Oladele IO, Omotosho TF, Adediran AA. Polymer-based composites: An indispensable material for present and future applications. *Int J Polym Sci.* 2020;2020:1–12. DOI:10.1155/2020/8834518.
67. Sanjay MR, Arpitha GR, Naik LL, Gopalakrishna K, Yogesha B. Applications of natural fibers and its composites: An overview. *Nat Res.* 2016;7(3):108–14. DOI:10.4236/nr.2016.73011.
68. Nwobi-Okoye CC, Uzochukwu CU. RSM and ANN modeling for production of Al 6351/ egg shell reinforced composite: Multi objective optimization using genetic algorithm. *Mater Today Commun.* 2020;22:100674. DOI:10.1016/j.mtcomm.2019.100674.
69. Pola A, Tocci M, Kapranos P. Microstructure and properties of semi-solid aluminum alloys: A literature review. *Metals.* 2018;8(3):181. DOI:10.3390/met8030181.
70. Chen L, Yao Y. Processing, microstructures, and mechanical properties of magnesium matrix composites: A review. *Acta Metall Sin (Engl Lett).* 2014;27(5):762–74. DOI:10.1007/s40195-014-0161-0.
71. Malaki M, Fadaei Tehrani A, Niroumand B, Gupta M. Wettability in metal matrix composites. *Metals.* 2021;11(7):1034. DOI:10.3390/met11071034.
72. Razzaq AM, Abdul Majid DLA, Ishak MR, M B U. A brief research review for improvement methods the wettability between ceramic reinforcement particulate and aluminium matrix composites. *IOP Conf Ser Mater Sci Eng.* 2017;203:012002. DOI:10.1088/1757-899X/203/1/012002.
73. Ren J-Y, Ji G-C, Guo H-R, Zhou Y-M, Tan X, Zheng W-F, Xing Q, Zhang J-Y, Sun J-R, Yang H-Y, Qiu F, Jiang Q-C. Nano-enhanced phase reinforced magnesium matrix composites: A review of the matrix, reinforcement, interface design, properties and potential applications. *Materials.* 2024;17(10):2454. DOI:10.3390/ma17102454.
74. Mishra D, Tulasi T. Experimental investigation on stir casting processing and properties of Al 6082/SiC metal matrix composites. In: *Advances in Composite Materials.* 2020. p. 159–68. DOI:10.1007/978-981-15-1124-0_14.
75. Singh AK, Soni S, Rana RS. Recent trends on furnace design and stirrer blade geometry used in stir caster: A focused review. In: *Advances in Composite Materials.* 2022. p. 147–59. DOI:10.1007/978-981-16-5371-1_14.
76. Abdallah A. Optimization of cutting parameters for surface roughness in CNC turning machining with aluminum alloy 6061 material. *IOSR J Eng.* 2014;4(10):1–10. DOI:10.9790/3021-041010110.

Disclaimer/Publisher's Note: The statements, opinions and data contained in all publications are solely those of the individual author(s) and contributor(s) and not of the publisher and/or the editor(s). This publisher and/or the editor(s) disclaim responsibility for any injury to people or property resulting from any ideas, methods, instructions or products referred to in the content.

© Copyright (2024): Author(s). The licensee is the journal publisher. This is an Open Access article distributed under the terms of the Creative Commons Attribution License (<http://creativecommons.org/licenses/by/4.0>), which permits unrestricted use, distribution, and reproduction in any medium, provided the original work is properly cited.

Peer-review history:

The peer review history for this paper can be accessed here:

<https://prh.ikpress.org/review-history/12375>